





Non-Linear Eddy Current Loss and Thermal Analysis on Transformer Cover

Mohammad Zia ZAHEDI^{1, 2,*} , Ires ISKENDER³ 

¹Electrical and Electronics Department, Engineering Faculty, Gazi University, Ankara, Turkey

²Physics Department, Electro-mechanic Faculty, Kabul Polytechnic University, Kabul, Afghanistan

³Electrical and Electronics Department, Engineering Faculty, Çankaya University, Ankara, Turkey

Article Info

Received: 21/06/2018

Accepted: 07/11/2018

Keywords

Eddy current losses
Finite difference method
Finite element simulation
Hot spot temperature
Transformer cover

Abstract

High current conductors of transformers cause to produce losses and thermal problems in their tank cover. Finite Difference (FD) Method (FDM) magnetic analysis is used to find out an exact estimation of the magnetic field and the losses near the bushings in the transient solution, considering the non-linear magnetic permeability of the cover plate, because FDM is more flexible to deal with the nonlinear constitutive law and easy-to-be implemented especially in the case of simple geometry. Finite Element Method (FEM) thermal analysis is used to determine the plate temperature based on magnetic FD analysis, taking account non-linear heat flux boundary condition. A calibration procedure is used between the analyses to ensure the precision of assumptions. The reliability of the technique, confirmed by experimental and FEM results.

1. INTRODUCTION

The eddy current losses in transformer cover plates due to high current of bushings degrades the insulating materials used in transformer. So it is vital to utilize advanced methods to find out an exact estimation of the magnetic field and eddy current losses in the steel plates [1-4].

Turowski has proposed a semi-analytical equation for losses calculation of the cover plate according to Poynting's theorem in both linear and nonlinear permeability [5, 6]. The linear magnetic analysis of the cover based on the solution of Maxwell's equations has been proposed by several authors using FEM [7-9], analytical method [10, 11] and FDM [12]. Recently, non-linear FEM [13], FDM [14] and analytical method [2] magnetic analysis has been done to obtain an accurate approximation of the cover losses using Poynting's theorem and Maxwell's equations, respectively. The non-linear magnetic FD analysis has been done in one dimension (1D) domain.

It is rather difficult to verify, experimentally, the eddy current losses obtained from the magnetic analysis because the direct measurement of the cover losses is not achievable. The cover plate thermal analysis has been proposed by authors using FEM [8, 13, 15, 16] and analytical solutions [17], in the coupling form of linear FEM-FEM [8], linear semi analytical-FEM [15] and nonlinear semi analytical-FEM [16] between eddy current loss and thermal analyses.

In addition, a calibration process has been applied to determine the magnitude of magnetic and thermal parameters to ensure the accuracy of numerical results [15, 16].

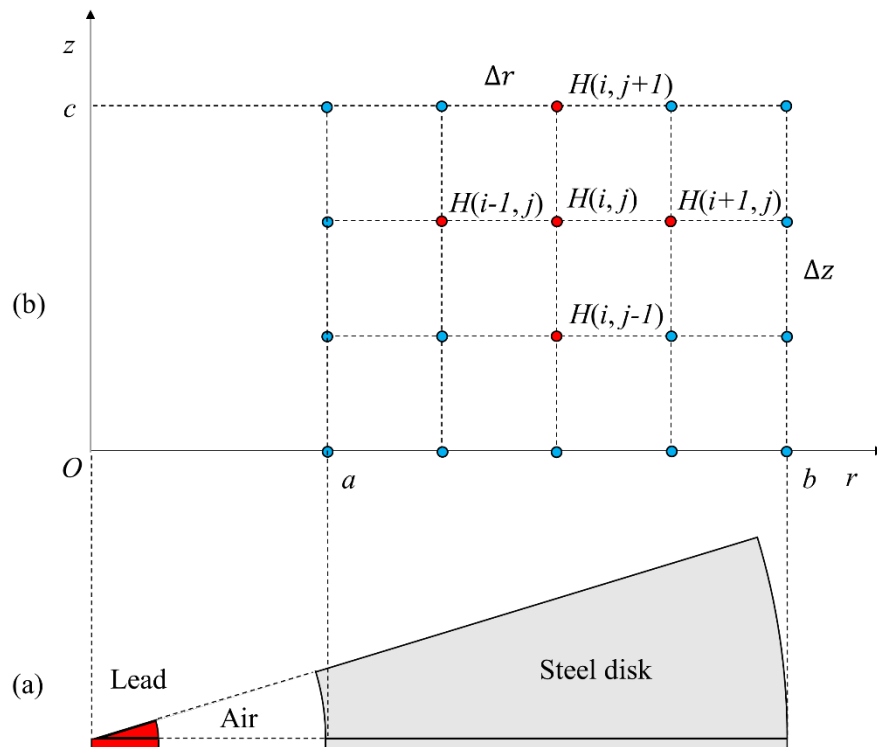


Figure 1. (a) The geometry, parameters, elements of the problem. (b) The computational stencil of the uniform FD mesh in magnetic analysis

FDM has advantages in comparison with FEM such as the FDM is easy to be implemented and easy to deal with the nonlinear constitutive law. Besides, FDM is the most common method used for solution domain with simple geometry. Therefore, for the simple geometry introduced in this study (2D) FDM Maxwell's equations based solutions of the magnetic field and losses at the bushing region of the transformers cover are used. The nonlinear behavior of the magnetic permeability of the steel and symmetry conditions of the solution area are considered in the given analysis. The proposed algorithm can be used to improve the transformers efficiency and their cover design, wherein it is not necessary to purchase special expensive software licenses and powerful computers. The temperature distribution of the cover is analyzed using non-linear 2D FEM thermal analysis. Finally, the calibration procedure which is based on the experimental data is performed on two analyses of FDM and FEM to ensure the precision of the results for the implemented parameters (natural convection coefficient, thermal conductivity and electrical conductivity) in the analyses.

2. PROPOSED METHODOLOGY

2.1. Magnetic Analysis Using FDM Approach

2.1.1. Linear Eddy Current Losses

The high current conductor passing through the bushings at low voltage side of transformer cover creates a variable magnetic field causing eddy current losses in the cover plate near the leads. Therefore, we can estimate the cover losses by taking account a disk steel with large enough radius and a long circular lead crossing perpendicularly the disk, as shown in Figure 1(a).

Magnetic analysis of the problem is done by (1), obtained from applying Ohm's law and Maxwell's equations in the disk as [11, 18].

$$\nabla^2 \mathbf{H} = \sigma \frac{\partial \mathbf{B}}{\partial t} \quad (1)$$

where \mathbf{B} , \mathbf{H} are flux density and intensity of the magnetic field, respectively, and σ is the electrical conductivity of steel plate.

Linear analytical solution of the disk losses is given by (2), considering only the radial component of eddy current density and neglecting the axial component due to its small value.

$$Loss_{bush} = \frac{I^2 q}{\pi \sigma} \ln\left(\frac{b}{a}\right) \cdot \left[\frac{\sinh(qc) - \sin(qc)}{\cosh(qc) + \cos(qc)} \right] \quad (2)$$

where I is the lead rms current, a , b and c are the internal radius, external radius and the thickness of the disk, respectively, according to Figure 1(a), and $q = 1/\delta$ where δ is the skin depth of disk steel and defined as:

$$\delta = \sqrt{2/\omega\mu\sigma} \quad (3)$$

where $\omega = 2\pi f$ is angular frequency of lead current and μ is magnetic permeability of steel [11].

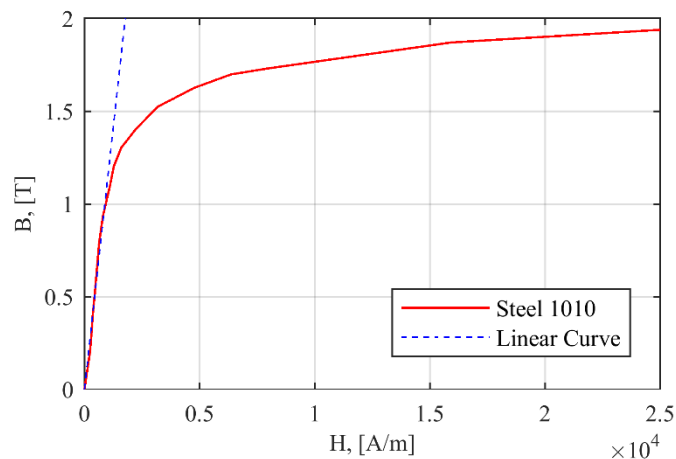


Figure 2. B - H curve for steel 1010 compared with a linear curve ($\mu_r = 900$)

2.1.2. Nonlinear Magnetic FD Analysis

The non-linear numerical solution of the magnetic field (1) can be done by applying B - H curve of the cover steel at each time interval of algorithm. The disk steel has the magnetization curve of steel 1010 taken from material library of ANSYS's program [19] as it has been used in [2, 11, 14, 20]. The relative permeability of 900 has been assumed in the case of linear analysis. A linear interpolation fitting method was used in deriving the B - H curve as (3).

$$H = f(B) \quad (4)$$

It is convenient to use (1) in a cylindrical coordinate system with a rectangular solution domain, at the cross section area in the axial symmetric page of the steel disk as shown in Figure 1(b), as (5).

$$\frac{1}{r} \frac{\partial H_\varphi}{\partial r} + \frac{\partial^2 H_\varphi}{\partial r^2} - \frac{H_\varphi}{r^2} + \frac{\partial^2 H_\varphi}{\partial z^2} = \sigma \frac{\partial B_\varphi}{\partial t} \quad (5)$$

where H_φ is the azimuthal, and the only, component of the magnetic field intensity vector \mathbf{H} [11, 18].

For 2D FDM analysis, we need to divide the solution region into an equally spaced grid of nodes with different mesh in z and r -directions. The steel thickness will be replaced with a grid of nodes which is equal to 10 times of skin depth number of thickness [14]. Therefore, for our configuration (Table 1) a grid of 66 points for the z -axis should be sufficient. It is not necessary to save all the computations on grid nodes during the work time of solution. FDM approximation of equation (5) can be given by:

$$B^{new}(i, j) = B(i, j) + \frac{\Delta t}{\sigma(\Delta r)^2} \left[\left(1 + \frac{\Delta r}{2r_i} \right) H(i+1, j) + \left(1 - \frac{\Delta r}{2r_i} \right) H(i-1, j) - \left(2 + \left(\frac{\Delta r}{r_i} \right)^2 \right) H(i, j) \right] + \frac{\Delta t}{\sigma(\Delta z)^2} [H(i, j+1) - 2H(i, j) + H(i, j-1)] \quad (6)$$

where $B(i, j)$ and $H(i, j)$ are the value of B and H on a grid node, $i=1, \dots, N_r$, $j=1, \dots, N_z$ for $N_r \times N_z$ point grid, $B^{new}(i, j)$ and $H^{new}(i, j)$ are the value of magnitude of magnetic flux density and magnetic field intensity at the next time step, respectively, $r_i = a + (i-1) \cdot \Delta r$ is the radial distance of mesh points, Δz and Δr are the distance between space points in z and r -directions, Δt is the time step [21].

Here, it should be noted that the following condition for time step determination should be satisfied with (6) to achieve a stable converged solution, considering $\Delta z \leq \Delta r$ due to small thickness and small penetration depth of steel cover.

$$\Delta t \leq \frac{\mu_{r,diff} \mu_0}{2} \sigma(\Delta z)^2 \quad (7)$$

where $\mu_{r,diff}$ is the relative differential permeability [22]. The time step may vary during process [14].

The Dirichlet boundary conditions (BCs) at $r = a$, $r = b$, $z = 0$ and $z = c$ surfaces are given by (8) which specify magnetic field intensity uniquely.

$$H(r, z) = I/2\pi r \quad (8)$$

At starting time of the solution $t = 0$, B and H values at all grid nodes are set to zero. At $t = \Delta t$, boundary values are set according to (7) and all the non-boundary values of $H(i, j)$ are still zero. The new values of magnetic flux density, $B^{new}(i, j)$, can be calculated using equation (6). $H^{new}(i, j)$ is given at all non-boundary nodes by (4). The solution algorithm usually continues for about 6 periods of oscillation time of the bushing current. Thus, at new time interval of $t + \Delta t$, magnetic field intensity at boundary condition $H(i, 1)$, $H(i, N_z)$, $H(1, j)$ and $H(N_r, j)$ are derived according to (8). The H values of other points changes from their initial values which is zero. Then, $B^{new}(i, j)$ are derived from (6) and the $H^{new}(i, j)$ for non-boundary points are determined using (4).

According to the fact that the time average eddy current losses can be found in the end of each cycle, the algorithm flowchart for eddy current losses calculations terminates when the losses error between two successive cycles is less than a given tolerance.

The eddy current density in the solution domain of the problem is determined by;

$$\mathbf{J} = -\frac{\partial H_\varphi}{\partial z} \hat{r} + \left(\frac{H_\varphi}{r} + \frac{\partial H_\varphi}{\partial r} \right) \hat{k} \tag{9}$$

For non-boundary nodes, a central difference approach in r -direction defined as following;

$$\frac{\partial H}{\partial r} = \frac{H(i+1, j) - H(i-1, j)}{2\Delta r} \tag{10}$$

For points on the $r = a$ surface ($i=1$) a second order difference approach defined as

$$\frac{\partial H}{\partial r} = \frac{-3H(1, j) + 4H(2, j) - H(3, j)}{2\Delta r} \tag{11}$$

At the other surface $r = b$ where ($i = N_r$) a second order difference approach defined as

$$\frac{\partial H}{\partial r} = \frac{3H(N_r, j) - 4H(N_r - 1, j) + H(N_r - 2, j)}{2\Delta r} \tag{12}$$

Second order differential type equations (11) and (12) are used to satisfy the required accuracy [14].

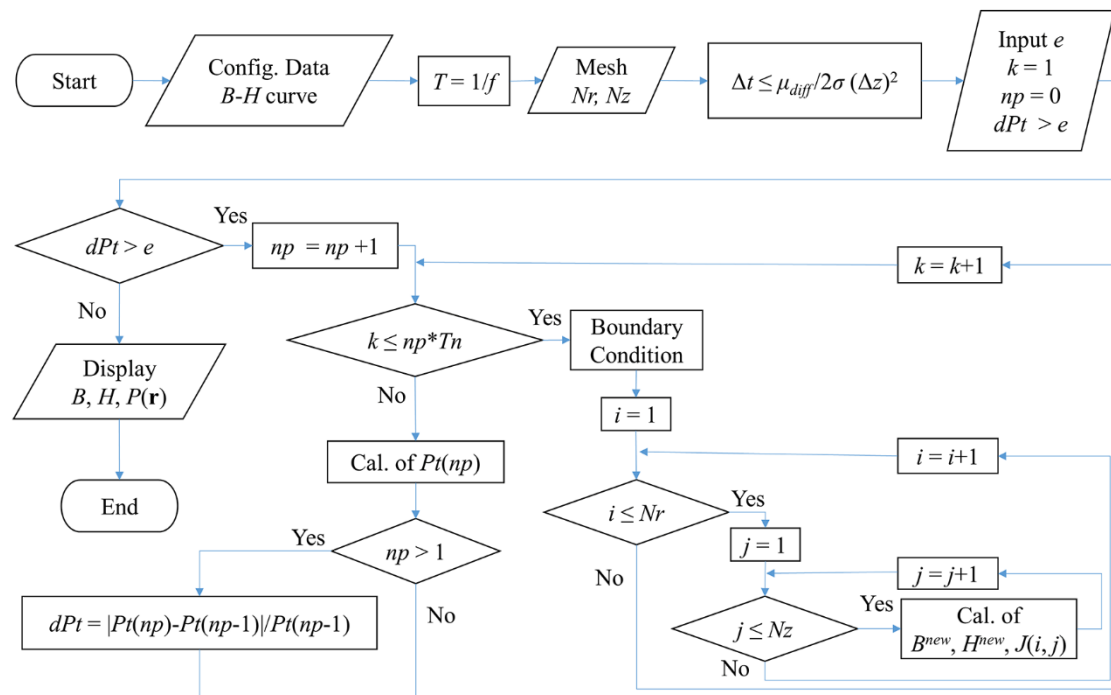


Figure 3. The flowchart of the FDM magnetic analysis

The time average eddy current losses of steel plate over a period can be determined as

$$Loss_{bush} = \frac{2\pi}{T\sigma} \sum_{k=1}^{k=T_n} \Delta t \sum_{j=1}^{j=N_z} \Delta z \sum_{i=1}^{i=N_r} |\mathbf{J}(i, j, k)|^2 r \Delta r \tag{13}$$

where \mathbf{J} is an instantaneous eddy current density at any points of grid and T is the cycle period.

Normally, the minimum value of differential permeability is given by using the peak of magnetic field intensity $I_m/2\pi a$ over a period from (8). Therefore, the time step can be defined according to (7). For some margin, the time step must be set lower [14].

Transient 2D FDM solution of the eddy current losses has been done according to the algorithm in Figure 3 with a programming tool like MATLAB. In this figure, e is the target tolerance of the eddy current losses between two successive period numbers, np is the number of period in which the calculations have been done and Pt is the eddy current losses at each period.

2.2. Non-Linear 2D FEM Thermal Approach

The last period of the transient solution of the losses has been exported to the 2D FE steady state or transient thermal model as heat source. Eddy current losses density $p_v(\mathbf{r})$ at any position \mathbf{r} of the solution domain obtained by (14)

$$p_v(\mathbf{r}) = \frac{1}{\tau} \int_0^\tau (J^2(\mathbf{r}, t) / \sigma) dt \quad (14)$$

where τ is the period of electromagnetic-field oscillation and J is the eddy current density.

Using axisymmetric condition of the problem, it is convenient to derive the equation of heat conduction [23] in a cylindrical coordinate system as (15), according to the technique used in [24] to reduce the three dimensions solution domain to 2D.

$$\rho C_p r \frac{\partial T}{\partial t} - \frac{\partial}{\partial r} \left(kr \frac{\partial T}{\partial r} \right) - \frac{\partial}{\partial z} \left(kr \frac{\partial T}{\partial z} \right) = r p_v \quad (15)$$

where k , ρ and C_p are thermal conductivity, density and specific heat of steel, respectively, and T is the temperature.

The hot spot temperature in the transient solution case can be determined as a function of time by (15). The heat conduction equation (15) at steady-state condition is simplified as (16).

$$-\frac{\partial}{\partial r} \left(kr \frac{\partial T}{\partial r} \right) - \frac{\partial}{\partial z} \left(kr \frac{\partial T}{\partial z} \right) = r p_v \quad (16)$$

where T is the final temperature of the plate as a result of equilibrium state.

Thermal boundary conditions of the problem are convective and radiative heat flux (17) on the disk surfaces, at $r = b$, $z = 0$ and $z = c$, and insulation boundary condition on the hole surface, $r = a$.

$$q = h_c (T - T_a) + \varepsilon_r \sigma_r (T^4 - T_a^4) \quad (17)$$

where h_c is the heat transfer coefficient, ε_r is the emissivity coefficient and σ_r is Stefan–Boltzmann constant.

Steady state and transient FEM thermal analysis have been developed in the Partial Differential equation (PDE) Tools of MATLAB, which solve PDEs, and it is possible to apply non-linear radiative and convective flux boundary condition according to the technique used in [25].

The required physical parameters in the magnetic and thermal analyses can be determined by using the calibration process for 1000A current. After calibration, FDM and FEM simulations are carried out for a different load current (500 A).

3. SIMULATION RESULTS

Table 1. The geometry and physical properties of the disk steel [26]

Parameter	Symbol	Value
Hole radius	A	30mm
Disk radius	B	50cm
Disk thickness	C	6mm
Ambient Temperature	T_a	21.8 °C
Steel relative permeability	μ_r	$B-H$ curve (Figure 2)
Steel relative permeability	μ_r	900
Steel electrical conductivity	σ	$6.8 \times 10^6 \text{ Sm}^{-1}$
Emissivity coefficient	ε	0.23
Steel thermal conductivity	k	$52 \text{ Wm}^{-1}\text{K}^{-1}$
Heat transfer coefficient	h_c	$5 \text{ Wm}^{-2}\text{K}^{-1}$

As a case study, the steel disk with the geometry and physical properties given in Table 1 [26] has been considered to verify the proposed 2D FDM. The copper lead has a radius of 24mm, a length of 1m, a magnetic permeability of $1 \times 4\pi \times 10^6 \text{ H/m}$ and an electrical conductivity of $58 \times 10^6 \text{ S/m}$. The AC current flows in the conductor is 500/1000 A, 50Hz.

The FDM magnetic analysis has been done at $N_z = 60$, $N_r = 300$ finite differences mesh in z and r -directions, respectively. The FDM waveforms of the magnetic field quantities of $H_\varphi(r, z, T/4)$ and $B_\varphi(r, z, T/4)$ have been calculated by (6) at instant $t = T/4s$ in the last period of the transient solution. The waveforms for 1000A current are shown in Figure 4 and Figure 5, for the grid points near the bushings.

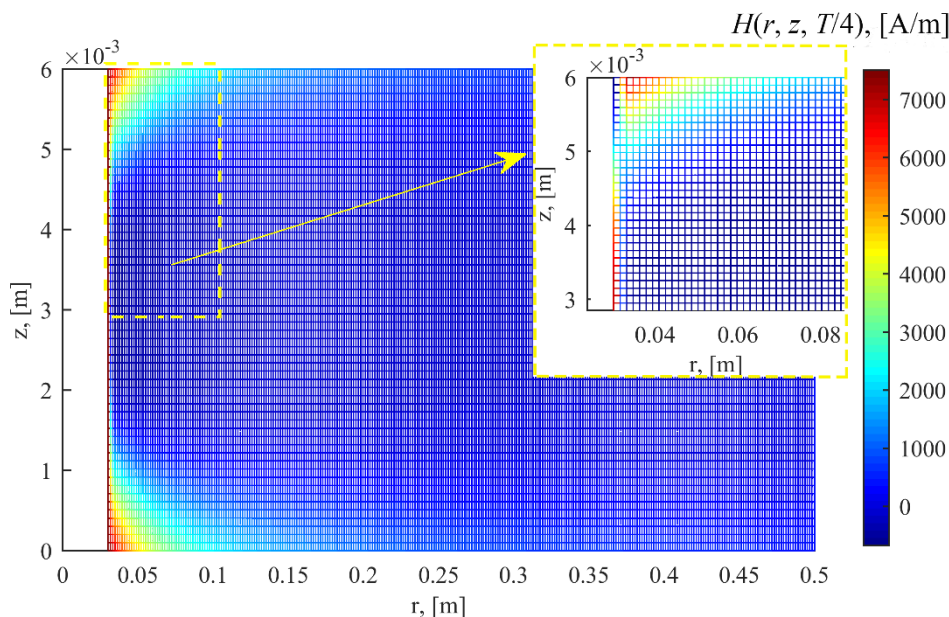


Figure 4. 2D FDM steady state waveforms of magnetic field intensity in the solution area and zoom-in near the conductor for 1000A

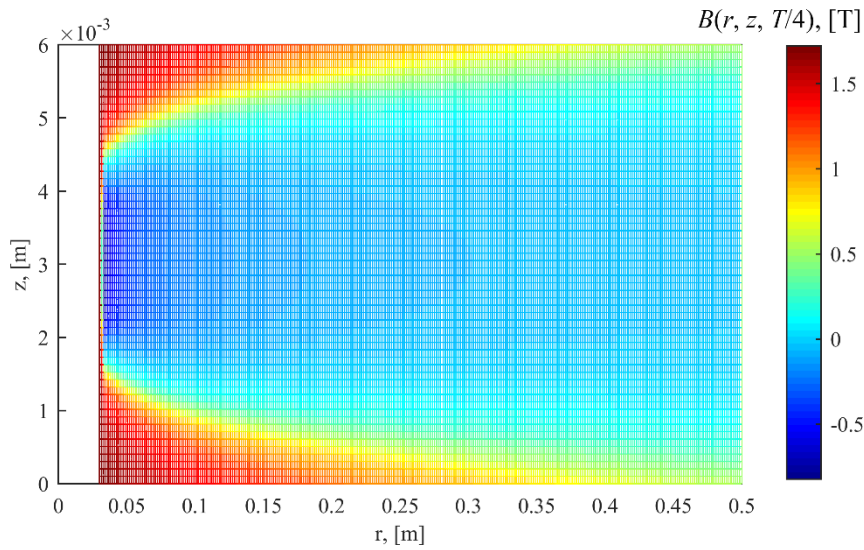


Figure 5. 2D FDM steady state waveforms of magnetic flux density in the solution area for 1000A.

The time average of the losses and losses density distribution on the grid nodes are determined by (13) and (14) during the last period of solution, as seen in the Table 2 and Figure 6, respectively. The non-linear 2D FDM transient solution of the disk losses, in the case of 1000A current, is shown in Figure 7. Eddy current losses of the disk for linear and non-linear magnetic permeability has been calculated by FDM, and the results have been compared with those of FEM and Analytical method in Table 2.

Table 2. Eddy current losses, [W] of the steel disk

Current, [A]	Linear, P _{total}			Non-linear, P _{total}	
	FDM	FEM	Analytic	FDM	FEM
500	36.6	36.8	36.06	34.1	31.5
1000	146.4	147.25	144.3	131.1	124.87

We can check the proposed method by calculating the eddy current losses at the constant magnetic permeability. The results are compared with those obtained from analytical method using (2) in Table 2. There is about 1.4% error, because of the applied mesh numbers (18000 FDs), which shows the efficiency of the method.

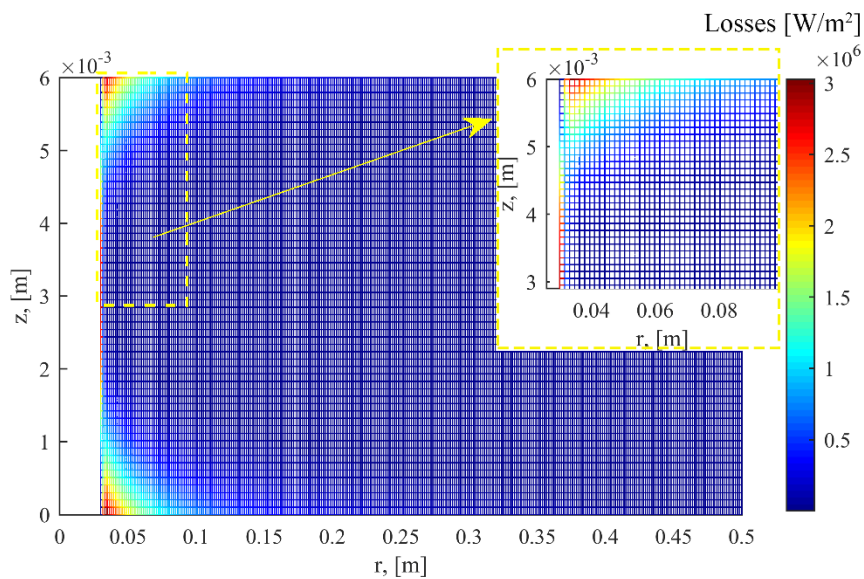


Figure 6. 2D FDM steady state waveforms of eddy current losses in the solution area and zoom-in near the conductor for 1000A

Transient hot spot temperature on the hole surface at $z = 3\text{mm}$ is presented in Figure 9, which shows in 3 hours reaches to the steady state condition.

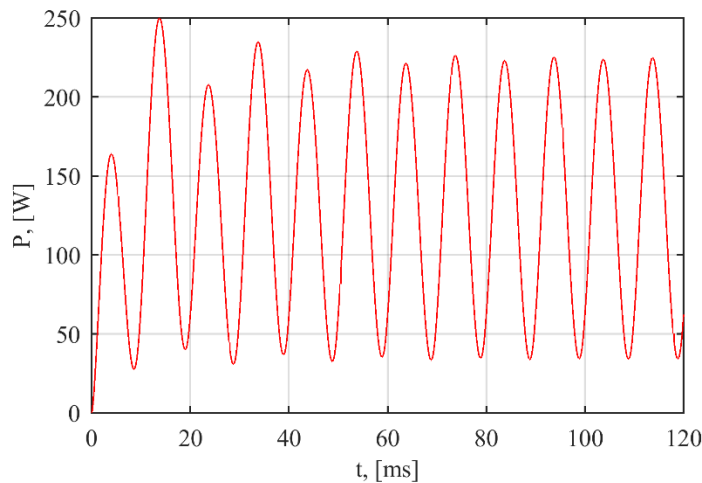


Figure 7. 2D FDM transient solution of the eddy current losses of the disk for 1000A

The results obtained from the non-linear FDM analysis are then compared with those of FE software like ANSYS. The FE model of the disk uses only 1/720 of the disk due to axial and azimuthal symmetries. The applied flux boundary conditions on the surface of the model are shown in Figure 8. A total of 36700 FEs done in the represented model. For accurate estimation of the magnetic field quantities and losses in the penetration depth of steel disk, the use of fine mesh is inevitable. It is sufficient to consider the skin effect of the disk 0.91 mm by setting four finite element layers of 0.227 mm on the disk surface at Maxwell's eddy current solution type.

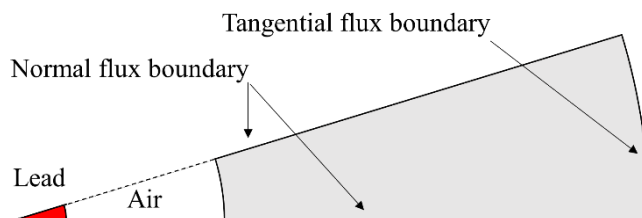


Figure 8. Flux boundaries of the tank cover model

The numerical method based estimated temperature values are given in Table 3, for two different cases of 500 and 1000 A current, at two solution points of ($r = a, z = 3\text{mm}$) and ($r = a, z = 6\text{mm}$). According to the results, the small absolute error between both methods verifies the FDM based solution. In addition, almost the same temperature along the thickness of the disk plate reveals that at the thermal analysis the cover thickness can be ignored.

Table 3. Hot spot temperature, [$^{\circ}\text{C}$] on the hole surface, $r = a$

Current, [A]	$z = 3\text{mm}$			$z = 6\text{mm}$		
	FDM	FEM	Abs. error	FDM	FEM	Abs. error
500	35.106	34.118	1	35.1	34.115	1
1000	67.59	67.678	-0.09	67.57	67.66	-0.09

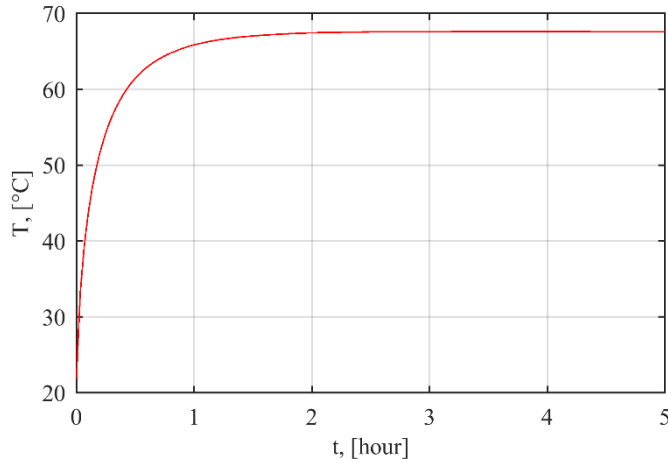


Figure 9. 2D FDM transient hot spot temperature on the hole surface at $z = 3\text{mm}$ for 1000 A

The FD transient and steady state temperature distribution on the cross section surface of the disk given in Figure 9 and Figure 10 have been calculated by the heat conduction equations (15) and (16), respectively. It can be observed in Figure 10 and Figure 11 that the FD temperature distribution of the disk is as well as FF based calculation.

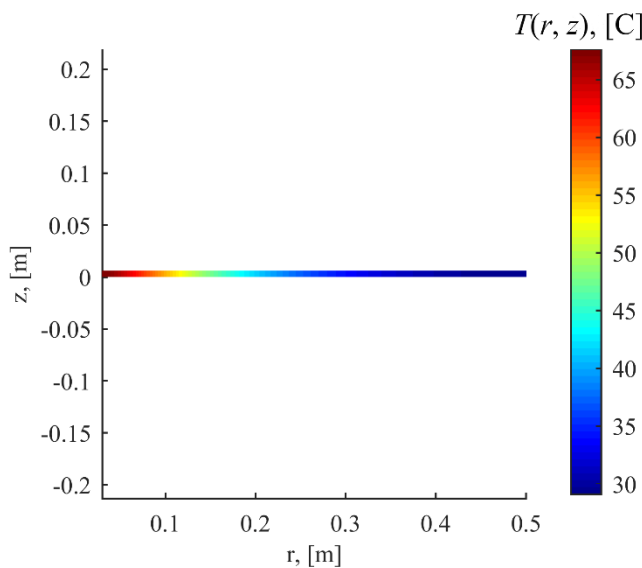


Figure 10. 2D FDM steady state temperature distribution, [°C], on the cross section surface of the disk for 1000A

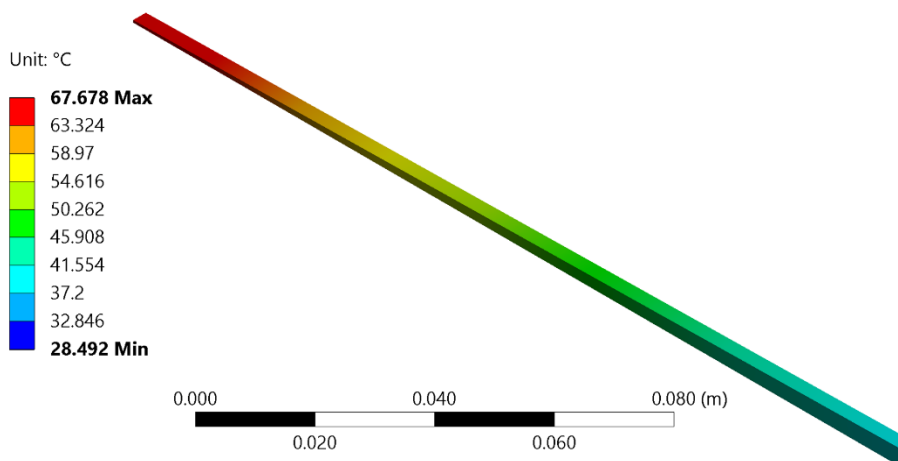


Figure 11. 3D FEM steady state temperature distribution on the section of the disk for 1000A

Linear and non-linear FDM temperature distributions in the center of the disk thickness, $z = 3\text{ mm}$, for bushing currents of 500 and 1000 A are presented in Figure 12. The results are verified by the experimental results [13, 15]. The FDM results has a better approximation in comparison with those of FEM, which verifies the non-linear FDM losses results in Table 2. According to Figure 12(a), the error of non-linear FDM and those of experiment is about -1.5°C for the case of 500A operation. The error between results of the non-linear FDM and those of experiments is about -0.03% , for the case of 1000A operation as shown in Figure 12(b). It is also observed in Figure 12(c) the difference between the temperature obtained by linear FDM and FEM is very small for the case of 1000A operation, as may be predicted from Table 2.

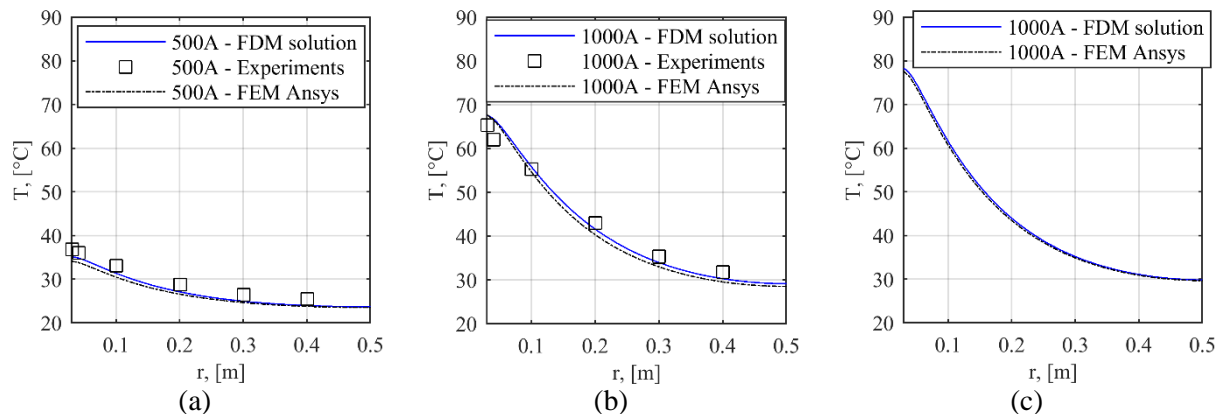


Figure 12. The temperature distribution of the disk plate obtained by the non-linear FDM, FEM and experiment for (a) 500A, (b) 1000A, and (c) by the linear FDM and FEM for 1000A

The another importance of comparing of linear and nonlinear cases for 1000A operation is that the error between nonlinear FDM and FEM with those of linear FDM and FEM is decreasing with increasing of magnetic fields. This is due to the fact that the $B-H$ curves of both linear and nonlinear operations for lower values of magnetic fields (far from the bushings) is very near to each other. For the higher values of magnetic field, the error between linear and nonlinear cases of operation is getting high and this is due to increasing of error of $B-H$ curves for higher values of the magnetic field. Though the error between linear and nonlinear cases is low for regions far from the bushings but the losses of these region are not considerable high and consequently is not important [5, 14].

4. CONCLUSIONS

Linear and non-linear magnetic FD analysis at the bushing regions of transformers cover studied in detail. The data of power losses obtained from the magnetic analysis has been imported into thermal heat conduction equation. Steady state and transient FEM thermal analysis are performed to determine the transformer cover temperature. Magnetic and thermal boundary conditions have been explained clearly. Non-linear radiative heat flux boundary condition has been considered in the study. Comparing results of 2D FDM for two different currents of 500 and 1000 A, with those of ANSYS and experiments show that the proposed methodology of FDM has a good and satisfied ability to be used in the non-linear analysis of the cover plate. Considering the accuracy and acceptable properties of the results, the easy usage and lower computational process of the proposed method makes it possible to use it in transformer design or research studies such as analyzing electromagnetic filed and eddy current losses in the windings and tank wall of transformers.

CONFLICTS OF INTEREST

No conflict of interest was declared by the authors.

REFERENCES

- [1] Kulkarni, S. V., Olivares, J. C., Perez, R. E., Lakhiani, V. K., and Turowski, J., "Evaluation of eddy current losses in the cover plates of distribution transformers", *IEE Proceedings - Science, Measurement and Technology*, 151(5): 313-318, (2004).
- [2] Maximov, S., Perez, R. E., Adame, S. M., Olivares, J. C., and Littlewood, E. C., "Calculation of nonlinear electromagnetic fields in the steel wall vicinity of transformer bushings", *IEEE Transactions on Magnetics*, 51(6): (2015).
- [3] Olivares, J. C., Georgilakis, P. S., and Ocon-Valdez, R., "A review of transformer losses", *Electric Power Components and Systems*, 37(9): 1046-1062, (2009).
- [4] Kulkarni, S. V. and Khaparde, S., *Transformer engineering: design, technology and diagnostics*, CRC Press, (2016).
- [5] Turowski, J. and Pelikant, A., "Eddy currents losses and hot-spot evaluation in cover plates of power transformers", *IEE Proceedings-Electric Power Applications*, 144(6): 435-440, (1997).
- [6] Turowski, J., *Elektrodynamika techniczna 2 nd ed.*, WNT, Warszawa, Poland, (1993)
- [7] Olivares, J. C., Perez, R. E., Kulkarni, S. V., Leon, F. D., and Vega, M. A. V., "2D finite-element determination of tank wall losses in pad-mounted transformers", *Electric Power Systems Research*, 71: 179-185, (2004).
- [8] Zahedi, M. Z. and Iskender, I., "3D FEM optimal design of transformer cover plates to decrease stray losses and hot spot temperature", *International Journal on Technical and Physical Problems of Engineering (IJTPE)*, 8(3): 56-60, (2016).
- [9] Olivares, J. C., Perez, R. E., Kulkarni, S. V., Leon, F. D., Vasquez, E. M., and Anaya, O. H., "Improved insert geometry for reducing tank-wall losses in pad-mounted transformers", *IEEE Transactions on Power Delivery*, 19(3): 1120-1126, (2004).
- [10] Maximov, S., Olivares-Galvan, J. C., Magdaleno-Adame, S., Escarela-Perez, R., and Campero-Littlewood, E., "New analytical formulas for electromagnetic field and eddy current losses in bushing regions of transformers", *IEEE Transactions on Magnetics*, 51: (2015).
- [11] Del Vecchio, R. M., Del Vecchio, R., Poulin, B., Feghali, P. T., Shah, D. M., and Ahuja, R., *Transformer design principles with applications: with applications to core-form power transformers 3 rd ed*, CRC press, (2017).
- [12] Zahedi, M. Z. and Iskender, I., "FDM electromagnetic analysis in bushing regions of transformer", *International Journal on Technical and Physical Problems of Engineering (IJTPE)*, 10(34): 27-33, Mar. (2018).
- [13] Lopez-Fernandez, X. M., Penabad-Duran, P., Turowski, J., and Ribeiro, P. M., "Non-linear heating hazard assessment on transformer covers and tank walls", *Przełąd Elektrotechniczny (Elect. Rev.)*, 88(7b): 28-31, (2012).
- [14] Vecchio, R. M. D. and Ahuja, R., "Analytic nonlinear correction to the impedance boundary condition", *IEEE Transactions on Magnetics*, 49(12): 5687-5691, (2013).
- [15] Fernandez, X. M. L., Duran, P. P., and Turowski, J., "Three dimensional methodology for the overheating hazard assessment on transformer covers", *IEEE Transactions on Industry Applications*, 48: 1549-1555, (2012).

- [16] Durana, P. P., Fernandez, X. M. L., and Turowski, J., "3D non-linear magneto-thermal behavior on transformer covers", *Electric Power Systems Research*, 121: 333-340, (2015).
- [17] Maximov, S., Escarela-Perez, R., Olivares-Galvan, J. C., Guzman, S. J., and Campero-Littlewood, E., "New analytical formula for temperature assessment on transformer tanks", *IEEE Transactions on Power Delivery*, 31(3): 1122-1131, (2016).
- [18] Sadiku, M. N., *Elements of electromagnetics*, Oxford university press, (2014).
- [19] "User's Guide - Maxwell 3D/ANSYS Maxwell 15 ed.", ANSYS Inc., Canonsburg, PA, USA, (2012).
- [20] Kumbhar, G. B., Mahajan, S. M., and Collett, W. L., "Reduction of loss and local overheating in the tank of a current transformer", *IEEE Transactions on Power Delivery*, 25(4): 2519-2525, (2010).
- [21] Sadiku, M. N. O., *Numerical techniques in electromagnetics*, CRC Press, New York, (2001).
- [22] Gillott, D. H. and Calvert, J. F., "Eddy current loss in saturated solid magnetic plates, rods, and conductors", *IEEE Transactions on Magnetics*, 1(2): 126-137, (1965).
- [23] Holman, J. P., *Heat transfer*, McGraw-Hill, New York, 1-5, (2010).
- [24] Internet: Heat distribution in a circular cylindrical rod, In MathWorks Online. https://www.mathworks.com/help/pde/examples/heat-distribution-in-a-circular-cylindrical-rod.html?s_tid=srchtitle, (2018).
- [25] Internet: Nonlinear heat transfer in a thin plate, In MathWorks Online. https://www.mathworks.com/help/pde/examples/nonlinear-heat-transfer-in-a-thin-plate.html?searchHighlight=Nonlinear%20Heat%20Transfer%20In%20a%20Thin%20Plate&s_tid=doc_srchtile, (2018).
- [26] Zahedi, M. Z. and Iskender, I., "Nonlinear Adaptive MagnetoThermal Analysis at Bushing Regions of a Transformers Cover Using Finite Difference Method", *Journal of Thermal Science and Engineering Applications*, 11(1): 011010-1 - 011010-8, (2018).